LEVEL II

*McCAULEY, HALPIN, EITELMAN, and HYNES

James W./McCauley, Bernard M./Halpin, Jr.,
Stephen D./Eitelman   Thomas V./Hynes

RADAR ABSORPTIVE MATERIAL FORM INDUSTRIAL EFFLUENT

JUN 1978

*JAMES W. McCAULEY, PhD
BERNARD M. HALPIN, JR., PhD
ARMY MATERIALS AND MECHANICS RESEARCH CENTER, WATERTOWN, MA   02172
STEPHEN D. EITELMAN, MR.
U.S. ARMY MATERIEL DEVELOPMENT AND READINESS COMMAND
ALEXANDRIA, VA   22333
THOMAS V. HYNES, PhD
ARMY MATERIALS AND MECHANICS RESEARCH CENTER, WATERTOWN, MA   02172

I.   INTRODUCTION

Recent innovative work (1,2) by the Nippon Electric Co. (NEC) Tokyo, Japan, on a ferrite precipitation method for removing heavy metal ions from industrial waste water and the subsequent potential use of this material (ferrite sludge) as a cheap microwave absorber has stimulated interest in the possible United States military applications of this concept. An important factor in this consideration is that the cost of the material is projected as significantly less than currently available ferrite material. This report describes the results of this program: a characterization and fabrication phase carried out at the Army Materials and Mechanics Research Center, Watertown, Massachusetts, and a testing phase carried out at the U.S. Army Electronic Proving Ground, Fort Huachuca, Arizona.

II.   MAGNETIC DIELECTRIC RADAR SIGNATURE REDUCTION

One way of reducing radar signatures of highly reflective materials is by the use of radar-absorbing coating materials. Magnetic dielectrics (ferrites) are a family of materials that can absorb microwaves by the lossy interaction of the electric and magnetic vectors of an electromagnetic wave with the material.

78 06 12 007

*McCAULEY, HALPIN, EITELMAN
and HYNES

When an electromagnetic wave strikes an object there is generally a reflection because of a discontinuity in electrical properties between the medium the wave is travelling and the object it strikes. One can show the following: an electromagnetic wave of amplitude E_O travelling in free space (μ [the magnetic permeability] = μ_O, and ϵ [the electrical permittivity] = ϵ_O) and striking a plane surface A ($\mu_A = \mu'_A + i\mu''_A$ and $\epsilon_A = \epsilon'_A + i \epsilon''_A$, where $\mu'_A \gg \mu''_A$ and $\epsilon'_A \gg \epsilon''_A$) will have a relection approximately $[1-[(\mu'_A/\epsilon'_A)(\epsilon_O/\mu_O)]^{\frac{1}{2}}$ in magnitude. If $\mu'_A/\epsilon'_A = \mu_O/\epsilon_O$, there will be no reflection. The wave will be attenuated in the material by a factor $\exp(-\mu''_A \omega[\mu'_A/\epsilon'_A]^{-\frac{1}{2}} \ell)$ where $\omega = 2\pi$ frequency and ℓ = the depth in the material. Thus by properly choosing the permeability, dielectric constant, depth, and loss factors, normal incident waves can be absorbed in the material. Unfortunately, however, all factors vary with frequency and this factor must be taken into consideration in the exact calculations. In this investigation, microwave attenuation and concomitant radar signature reductions have been achieved by an increase in the magnetic permeability and magnetic losses of a dielectric material.
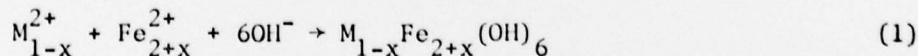
III. DESCRIPTION OF FERRITE PRECIPITATION PROCESS

Stimulated by more stringent pollution control requirements in Japan, the NEC is investigating the use of a ferrite precipitation process to remove heavy metals from their industrial waste water (1). They have two motives for exploring this unique idea: (1) purification of industrial waste water and (2) simultaneous formation of significantly cheaper ferrite raw material for possible commercial use. Potential uses envisioned by them include prevention of double TV images (ghosts) by using ferrite coatings on buildings and also elimination of ground reflections near radar receivers by coating the ground.

Standard industrial practice (3) used in the production of ferrite materials consists of elaborate mixing, pressing, and controlled heat treatments of carefully weighed, mechanically pulverized, and mixed ceramic oxide powders. The novel technique being used by NEC is a wet chemical reaction process referred to as coprecipitation. Essentially, divalent iron and other metal ions are hydrolyzed in a basic solution and then oxidized into the ferrite spinel structure (2).

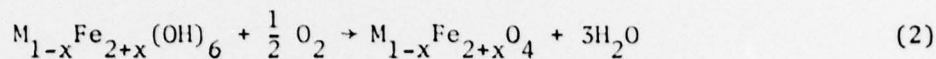The two steps can be formularized as follows:

Hydrolysis:

$$M^{2+}_{1-x} + Fe^{2+}_{2+x} + 6OH^- \rightarrow M_{1-x}Fe_{2+x}(OH)_6 \tag{1}$$

Warm Aeration:

$$M_{1-x}Fe_{2+x}(OH)_6 + \frac{1}{2} O_2 \rightarrow M_{1-x}Fe_{2+x}O_4 + 3H_2O \qquad (2)$$

or more simply as

$$Fe^{2+} + M^{2+} + ROH + O_2 \rightarrow M_{1-x}Fe_{2+x}O_4 \qquad (3)$$
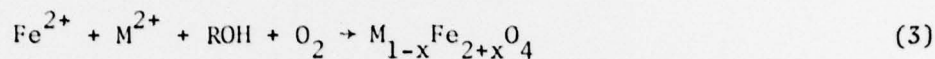
where R = alkali or alkali earth cation (ex. NaOH).

In summary, the ferrite sludge coprecipitation process is schematically illustrated in Figure 1.
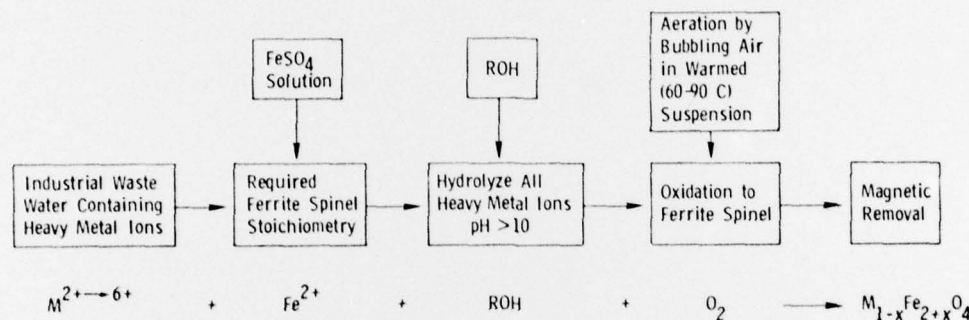

Figure 1. Schematic flow chart for the production and removal of ferrite sludge by the coprecipitation process.

Experimental data demonstrate that the heavy metal removal technique is successful. Table 1 lists various heavy metal ions in the industrial waste water before and after the coprecipitation treatment (1).

IV. CHARACTERIZATION OF FERRITE SLUDGE

Two separate batches of sludge, nominally referred to as the 5-kg and 50-kg batches, were obtained from NEC. They were brown to dark brown in color and had a mud-like consistency. Figure 2 illustrates both the as-received material and also the dried, ball-milled, and sieved (-325 mesh) powder.

Table 1. HEAVY METAL ION CONCENTRATIONS IN INDUSTRIAL WASTE WATER BEFORE AND AFTER FERRITE SLUDGE COPRECIPITATION TREATMENT.

Heavy Metal Ion	Concentration in Waste Water (ppm)	
	Before Treatment	After Treatment
Cu	9,500	< 0.5
Ni	20,000	< 0.5
Sn	4,000	<10
Pb	6,800	< 0.1
Cr^{6+}	2,000	< 0.1
Cd	1,800	< 0.1
Fe	over 1%	< 1.0
Hg	3,000	ND*

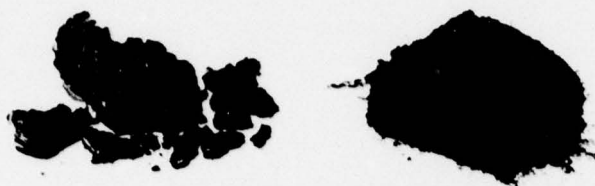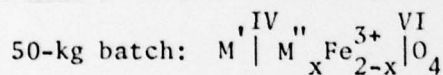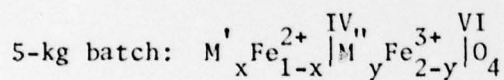*Nondetectable

Figure 2. Ferrite sludge.

AS RECEIVED

DRIED, BALL MILLED,
AND SIEVED

The as-received sludge contains appreciable amounts of water and must be thoroughly dried prior to further use. Table 2 lists the water content and approximate chemistry of the two batches which are quite different in composition, the 5-kg batch being iron-rich and the 50-kg batch being iron-poor.

Hypothetical chemical-structural formulas for these ferrite spinels are as follows (4,5):

5-kg batch: $M'_x Fe^{2+}_{1-x} |M''_y Fe^{3+}_{2-y}|^{VI} O_4$

50-kg batch: $M' |M''_x Fe^{3+}_{2-x}|^{VI} O_4$

M', M'' = heavy metal ions,

IV, VI = tetrahedral and octahedral

coordination, respectively.

Table 2. CHEMISTRY OF AS-RECEIVED FERRITE SLUDGE

Element	Weight Percent in Batches	
	5 kg	50 kg
H_2O*	45.0	43.9
Fe†	65.7	49.2
Mn‡	0.5-1	1
Mg	.5	1
Al	.1-0.5	1
Ni	.5	1
Si	.5	1-10
Pb	.1-0.5	0.5-1
Sn	.05	.5
Zn	.1	.5-1
Cr	.01	.5
Ca	.1	.5
Cd	.5	.5
Cu	.05	.05-0.1
Mo	.05-0.1	.05-0.1
Ti	.01-0.05	.1-0.5
Zr	.05	.05
Ba	.05	.05

*Loss on drying at 105 C.
†Quantitative analysis for Fe by wet chemistry
‡All the remaining analysis are semiquantitative emission spectroscopic results reported in weight percent

There are eight formula units in the ferrite spinel unit cell, yielding the following actual chemical formula: $M'_8 M''_{8x} Fe_{16-8x} O_{32}$.

Hence, there are at least $M'_8 + M''_{8x}$ crystallographic sites in the unit cell for the removed heavy metal ions.

Figure 3 is a diagrammatic representation of the actual powder diffraction patterns using filtered CrKα radiation. The 5-kg batch is 100% ferrite with a $LiFe_5O_8$ (ferrite)-like structure. The 50-kg sludge is a relatively impure ferrite sample containing several nonferrite phases. Roughly 60% of the mixture is a ferrite similar to $LiFe_5O_8$,

*McCAULEY, HALPIN, EITELMAN
and HYNES

3% is $Fe(OH)_3$, 6% is $ZnCr_2O_4$ (spinel), 11% is NiO, and the last 20% consists of $FeCl_3$, $CaSnO_4$, and $CaFeO_7$ (ferrite). It is also possible that a significant percentage of both batches contain X-ray amorphous phases and therefore do not appear in the diffraction patterns.

Table 3 lists the physical powder characteristics of the two batches. Figure 4 illustrates a high magnification view of the 5-kg powder, showing its very fine grain size. The 5-kg batch is a higher density, larger grain size material than the 50-kg material. Ideal densities for ferrites of similar chemistry as reported here are about 5.0 g/cc, close to the 5-kg material, but significantly different than the 50-kg material. All these data indicate that the 5-kg powder more
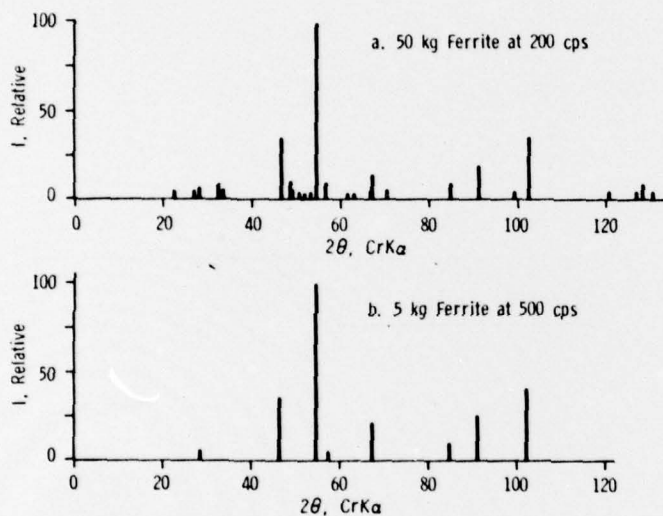

Figure 3. X-ray powder diffraction patterns (CrKα) of two dried, ball-milled, and sieved (-325) ferrite sludge powders; CrKα radiation.

Table 3. POWDER CHARACTERISTICS OF FERRITE SLUDGE

Drying Conditions: 150 C, 24 hr

Type kg	Heat Treatment T°C	t(hr)	Atm	Surface Area* m^2/g	Equivalent Spher. Diam.+ μm	ρ_0+ g/cc
5	-	-	-	20.83	0.058	4.88
5	480	24	Air	16.12	0.075	-
5	480	72	Air	14.26	0.084	-
50	-	-	-	29.97	0.040	3.81
50	400	26	Air	23.77	0.050	-
50	400	136	Air	23.11	0.052	-

*By a BET technique
+Equivalent spherical diameter assuming a density of 5.0 g/cc
‡Measured density by a helium-air pycnometer method

Figure 4. SEM photomicrograph of fracture surface of ferrite sludge powder cold isostatically pressed at 20,000 psi and heat treated for 24 hr at 200 C.

nearly represents a ferrite material, whereas the 50-kg material is a very impure ferrite powder, suggesting that the NEC process will not yield identical material. However, the ferrite sludge in both cases is a magnetic ferrite, and no heat treatment is required to form a ferrite phase as in conventional ferrite manufacturing processes. Further, there seems to be a direct correlation between the iron content and the ferrite content of the two batches. This implies that enough $FeSO_4$ must be added to coprecipitate all the heavy metals in a ferrite phase, otherwise the hydrolysis and warm aeration will produce other nonferrite material.

V. FABRICATION PROCEDURE

Three processing routes were analyzed for use in the production of the large 12" × 12" testable sample tiles:

    a. pressed powder, no heat treatment,
    b. sintered powder, and
    c. organic matrix composite.

Prior work by the NEC implied that either a or b was sufficient for wave guide (VSWR) microwave absorption measurements on small samples (6-8). However, because of our remote test location and large sample requirements for radar absorption measurements only methods b and c were considered practical. In order to decide between these procedures a preliminary thermal analysis and sintering study was carried out on the two batches.

*McCAULEY, HALPIN, EITELMAN
and HYNES

a. Thermal Analysis

Initial sintering runs clearly demonstrated a complex sequence of reactions and densification characteristics, the major problem being the oxidation of the ferrite to the nonmagnetic α-Fe_2O_3 (hematite) phase. The reaction can be simplified as follows:

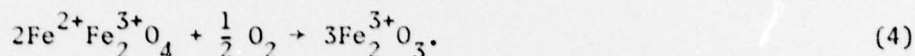$$2Fe^{2+}Fe_2^{3+}O_4 + \frac{1}{2}O_2 \rightarrow 3Fe_2^{3+}O_3. \tag{4}$$

Figure 5 illustrates the thermogravimetric analysis (TGA) curves for the two batches and Figure 6 shows the differential thermal analysis (DTA) traces of heat-treated and untreated samples. Apparently, because of excessive volatilization of nonferrite metal oxide phases, the TGA curves show weight losses and not weight gains as would be expected for reaction (Eq. 4). However, the DTA curves clearly show the α-Fe_2O_3 reaction at about 604 C in the 5-kg material (Figure 6a) and roughly 340 C in the 50-kg material (Figure 6b). This was confirmed by X-ray diffraction analysis of resultant products. In an attempt to stabilize the ferrite spinel structure, extended heat treatments were carried out below the transformation temperature. The DTA curves for these heat-treated samples (Figures 6c and 6d), however, again show the α-Fe_2O_3 transformation. Clearly, heat treatment in air above the
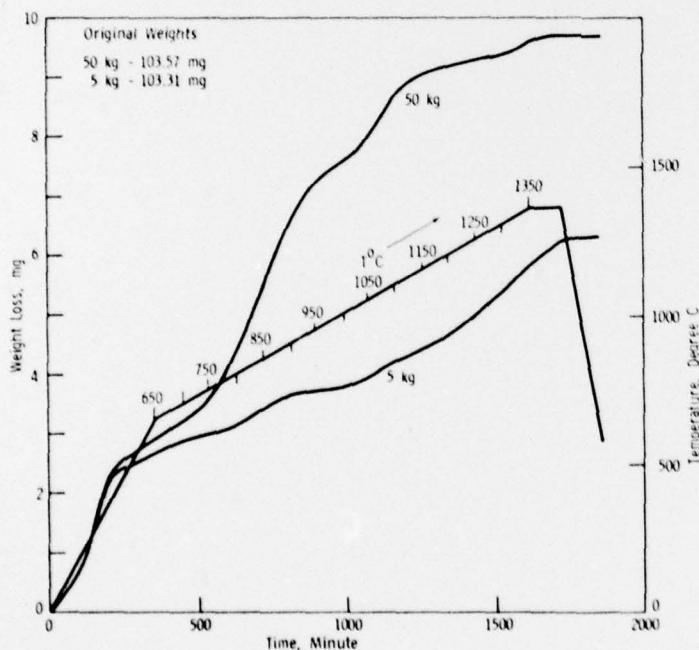

Figure 5. Thermogravimetric analysis traces of predried and pressed ferrite sludge powder.
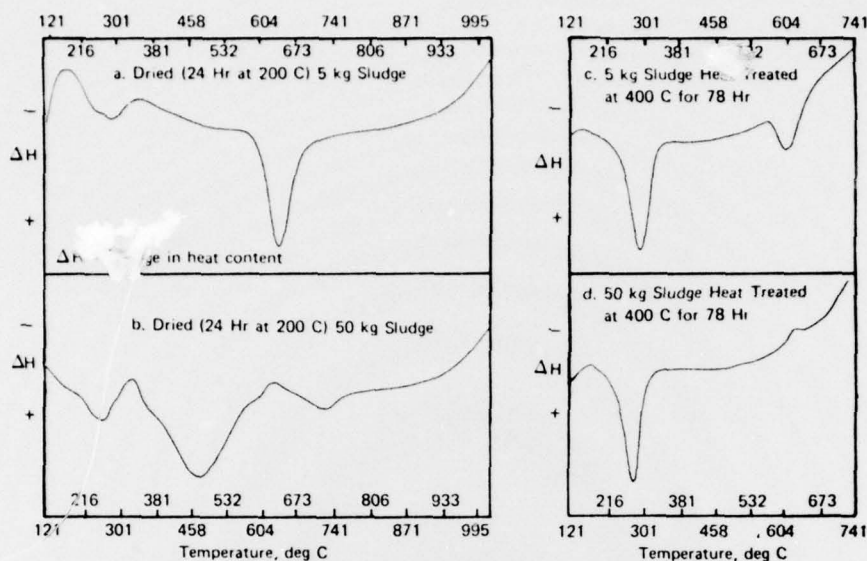
Figure 6. Differential thermal analysis heating curves of
ferrite sludge powders - all heated in air.

α-Fe_2O_3 transformation temperature always results in an α-Fe_2O_3 product
which is unacceptable. One additional DTA experiment using flowing
argon instead of air confirmed this deduction.

b. Sintering Studies

Preliminary sintering work was also carried out with a
summary of the data plotted on Figure 7, showing the variation of
observed densities as a function of temperature. The data simply
reflects the oxidation of the ferrite sludge to α-Fe_2O_3 and its sub-
sequent densification. All samples were isostatically cold pressed
at 20,000 psi prior to heat treatment. Scanning electron microscope
(SEM) photomicrographs of fracture surfaces of runs labeled 18, 23,
and 24 in Figure 7 are presented in Figure 8. As can be seen, sinter-
ing in flowing air results in a completely α-Fe_2O_3 body (Figure 8b),
whereas sintering in argon or a limited amount of air results in a
sintered ceramic containing ferrite (Figure 8a and 8c). Figure 9
shows the microstructural details of the precipitation of α-Fe_2O_3 from
a ferrite matrix. This sample was dried at 200 C for 24 hours and then
heat treated at 1200 C for 24 hours in air. All these data indicate
that the production of large fully-sintered ferrite ceramic tiles must
be preceded by an in-depth atmosphere-controlled sintering study, which
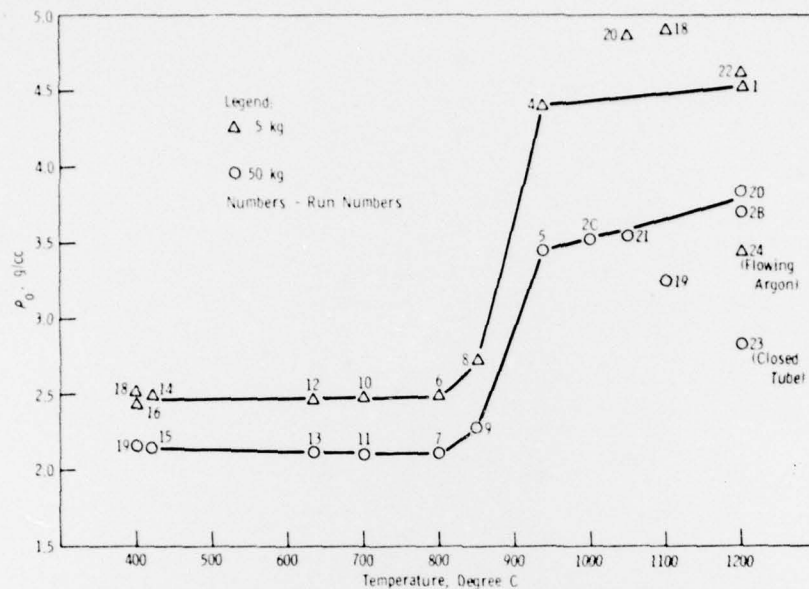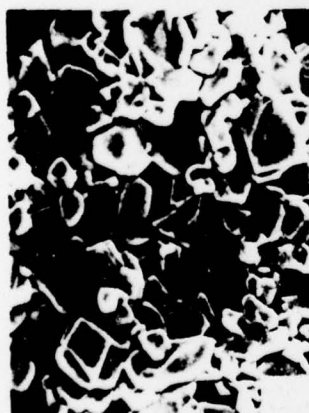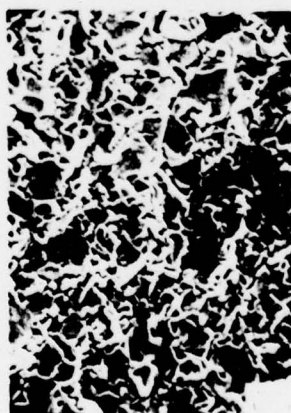was deemed prohibitively expensive as a processing procedure.

8

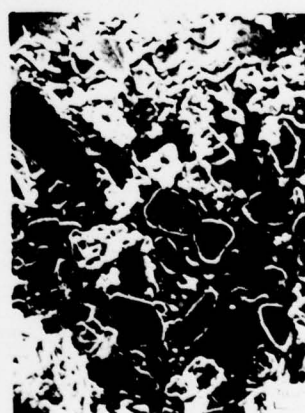Figure 7. Variation of observed density of heat-treated ferrite sludge powder.

a. 100% Ferrite: Calcined in Air at 487 C for 22 Hr, Sintered at 1200 C for 4 Hr in Flowing Argon

(Run 24)

b. 100% α-Fe$_2$O$_3$: Calcined in Air at 400 C for 78 Hr, Sintered at 1100 C for 40 Hr in Air

(Run 18)

c. 22% Ferrite, 78% α-Fe$_2$O$_3$: Calcined in Air at 400 C for 48 Hr, Sintered at 1200 C for 4 Hr in Closed Muffle Tube

(Run 23)

Figure 8. SEM photomicrographs of representative fracture surface microstructures of heat-treated ferrite sludge powders.

Figure 9. SEM photomicrograph of fracture surface of ferrite sludge heat treated at 1200 C in air for 24 hours. Microstructure of precipitation of lenticular α-Fe_2O_3 from ferrite matrix.

c. Feasibility of Organic Matrix

It was very quickly demonstrated that at least 50 wt% ferrite powder (-325 mesh) could easily be incorporated into an EPON 828/Z curing agent (100 parts/20 parts) epoxy resin matrix. The powder was not rejected by the resin and formed a homogeneous ferrite/resin composite material and did not lose its magnetic properties.

VI. PRODUCTION OF FERRITE/RESIN TILES

A special mold was constructed to form, de-gas, and cure the ferrite/resin composite. Additionally, it was designed to have a 1/16" overhang of resin over the Al backup plate to prevent direct exposure of the Al plate to the microwave signals, even in a slightly tilted situation. The following is a summary of the final fabrication process.

a. Dry at 150 C and ball mill for at least 24 hours.

b. Sieve all powder through -325 mesh screen.

c. Mechanically blend 50 wt% ferrite powder in an EPON 828/Z curing agent resin mixture.

d. Casting procedures:

(1) Self-bonding

(a) De-gas ferrite/resin mixture.

(b) Cure 2 hr at 175 F, 2 hr at 300 F, directly to Al backup plate.

10

        (2) Two-step process

        (a) De-gas ferrite/resin mixture.

        (b) Cure 4 hr at 175 F using a mold release on Al backup plate.

        (c) Bond to Al backup plate using a two-part Epoxy Adhesive 907.

    e. Grind ferrite/epoxy surface to final required thickness dimension.

Four composite plates were fabricated and described in Table 4. Samples FP-1 through FP-4 were all bonded to 12" × 12" × 5/16" Al plates; the ferrite/resin composites measured 12-1/8" × 12-1/8". Side views of these test panels can be seen in Figure 10.

Figure 10. Photograph of four test tiles and standard Al plate - side view.

Table 4. DESCRIPTION OF FERRITE/RESIN COMPOSITE PLATES

Sample	Ferrite	Resin Thickness	Process
FP-1	Undoped	1/8"	1 step
FP-2	50 kq-50 Wt%	1/8"	1 step
FP-3	50 kq-50 Wt%	3/8"	2 step
FP-4	5 kq-50 Wt%	1/8"	2 step
FP-5	Blank Al Plate		

VII. MICROWAVE ABSORPTION TESTS

The microwave absorption tests were carried out by Captain
J. Newton, Mr. K. Hakes, Mr. W. Krotzer, and Warrant Officer G.
Van Horn at the Electromagnetic Interference Laboratory, Black Tail
Canyon Test Facility, U.S. Army Electronic Proving Ground, Fort
Huachuca, Arizona. Figure 11 is a drawing of the actual arrangement
of the test panel, receiving antenna, and transmitting horn used in
this experiment. After several unsatisfactory series of measurements
using either a wood or lucite test panel holder, a target holder con-
sisting of a styrofoam block with a recess cut to hold the test panels
was selected for the final measurements.
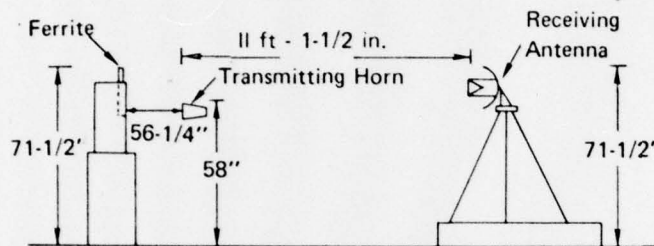

Figure 11. Physical arrangement of microwave test equipment
and test plate in Fort Huachuca anechoic chamber.

Average ΔdB (difference between the standard uncoated Al plate
and ferrite/resin coated plates) and equivalent percent absorption for
the various test panels are plotted against frequency in Figure 12.
Also plotted on the figure are the common radar bands of interest.
All the microwave measurements were repeatable within 1.5 dB. There
is significant attentuation of the microwave signals by the 50-kg
3/8"-thick ferrite/resin composite in two regions: about 5 dB absorp-
tion (68%) in the 3 to 4.5 GHz region and over 6 dB absorption (75%)
in the 10 to 13 GHz J-band region. There also seems to be small ab-
sorptions at about 7 and 8 GHz. All three ferrite-treated resins show
similar effects, the 3/8"-thick composite with the impure 50-kg fer-
rite exhibiting the most pronounced. However, from 4 to 8 GHz a small
enhancement in attenuation of the 5-kg (pure) ferrite over the 50-kg
(impure) ferrite did seem to occur. In general, there was a negligible
dependence of absorption on the purity of the ferrite powder, suggest-
ing that the Fe content of the sludge could be significantly reduced
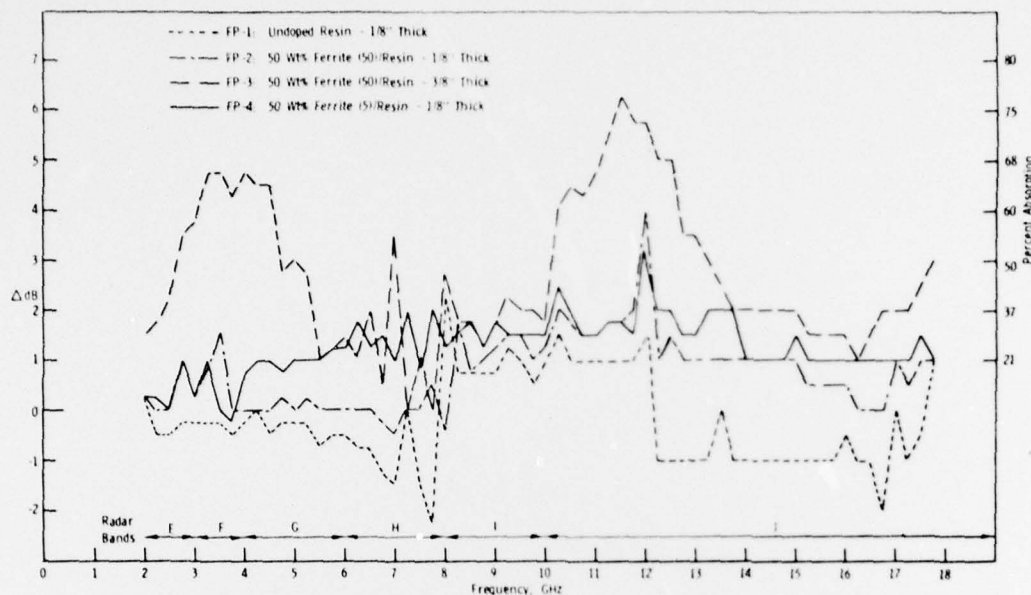without appreciably affecting the radar absorption properties.

Figure 12. Graphical results of microwave absorption tests of ferrite/resin composites;
difference in amplitude from Al plate (ΔdB) plotted against frequency (GHz).

VIII. SUMMARY AND CONCLUSIONS

A comprehensive study has been carried out to evaluate the
microwave absorption potential of a ferrite sludge derived by a copre-
cipitation treatment of industrial waste water. Full characterization
of two different batches of sludge showed quite different chemistries,
especially in the amount of iron content; one was iron-rich, the other
iron-poor, differing by about 15% to 16% Fe. The iron-rich ferrite
was determined to be 100% ferrite spinel, whereas the iron-poor ferrite
was only 60% ferrite. The powders have an extremely fine grain size
with a surface area of 20 to 30 m^2/g, indicative of an average equiva-
lent spherical diameter of about 0.05 μm. Careful thermal analysis
and sintering studies clearly demonstrated that only carefully con-
trolled atmospheres can be used to sinter the ferrite sludge powder
into a mechanically coherent ferrite ceramic. The major problem is
the oxidation of the ferrite to the nonmagnetic α-Fe_2O_3 (hematite)
phase at relatively low temperatures. Because of these constraints a
ferrite/resin (EPON 828/Z) composite system was selected as the most
appropriate material configuration for the microwave absorption
evaluation of the sludge. Microwave testing of four test panels in
the Fort Huachuca anechoic chamber demonstrated significant attenuation
of the microwave signals by a 3/8"-thick ferrite/resin composite in two

regions: 3 to 4.5 GHz (68%) and 10 to 13 GHz (75%). There seemed to be no significant difference in results using either the iron-rich or iron-poor ferrite sludge material, showing that significantly less iron could be used in the ferrite coprecipitation waste water treatment process.

The data obtained in our investigation and the unconfirmed results of NEC strongly suggest that the ferrite sludge concept could prove to be an important new method of inexpensively reducing radar signatures, by either a coating technique or smoke generation, while stimulating the ecologically important purification of industrial waste water. Also the possibility exists that the fundamental concept confirmed in this program could be further optimized. Moreover, it is our conclusion that the fabrication of massive fully sintered radar-absorbing ceramic ferrites would prove prohibitively expensive and unjustifiable from a practical point of view. Instead, the organic-based matrix concept seems to be the most practical and feasible at this point, as well as the use of the ferrite powder in camouflage smokes.

IX. ACKNOWLEDGMENTS

*McCAULEY, HALPIN, EITELMAN
and HYNES

REFERENCES

1. ASAI, G. N. *Research Planned by Nippon Electric Co., Ltd., on
    the Prevention of Electromagnetic Wave Reflection by the Use of
    Ferrite Sludge.* U.S. Army Foreign Science and Technology Center,
    Report 2-253-0111-74, February 1974.

2. TAKADA, T., and KIYAMA, M. *Preparation of Ferrites by Wet Method:
    Ferrites* in Proceedings of the International Conference, ed.,
    Y. Hoshino, S. Iida, and M. Sugimoto, University Park Press,
    Tokyo, Japan, 1970.

3. PAULUS, M. *Preparation Conditions of the Ferrites* in Prepara-
    tive Methods in Solid State Chemistry, ed., P. Hagenmuller,
    Academic Press, New York, 1972, p. 487-531.

4. GRAY, T. J. *Oxide Spinels* in High Temperature Oxides - Part IV,
    Refractory Glasses, Glass-Ceramics, and Ceramics, ed., A. M.
    Alper, Academic Press, New York, 1971, p. 77-107.

5. BLASSE, G. *Crystal Chemistry and Some Magnetic Properties of
    Mixed Metal Oxides with Spinel Structure.* Philips Research
    Reports Supplements, no. 3, 1964, 139 pages.

6. ASAI, G. N. *Research on Treatment and Properties of Ferrite
    Sludge for Microwave Absorption.* U.S. Army Foreign Science and
    Technology Center, Report 2-253-0593-75, 12 August 1975, (FOUO).

7. AKASHI, T., SUGANO, I., OKUDA, T., and TSUJI, T. *Sintering of
    Coprecipitated Manganese Zinc Ferrite Powder: Ferrites* in
    Proceedings of the International Conference, ed., Y. Hoshino,
    S. Iida, and M. Sugimoto, University Park Press, Tokyo, Japan,
    1970.

8. AKASHI, T., SUGANO, I., KENMOKU, Y., SHINMA, Y., and TSUJI, T.
    Low-Loss and High-Stability Mn-Zn Ferrites in Proceedings of
    the International Conference, ed., Y. Hoshino, S. Iida, and
    M. Sugimoto, University Park Press, Tokyo, Japan, 1970.

15